Nanocrystals

DOI: 10.1002/anie.200902235

Twin-Induced Growth of Palladium–Platinum Alloy Nanocrystals**

*Byungkwon Lim, Jinguo Wang, Pedro H. C. Camargo, Claire M. Cobley, Moon J. Kim, and Younan Xia**

The physicochemical properties of a metal nanocrystal are highly sensitive to its shape,[1] which is mainly determined by the internal crystal structure (i.e., twinned vs. single-crystal).[2] Notable examples of shapes that have been observed for metal nanocrystals include fivefold twinned decahedrons and icosahedrons,[3,4] singly twinned right bipyramids,[5] and thin plates with lamellar twins,[6,7] as well as single-crystalline cubes and truncated octahedrons.[8] Nanocrystals with twinned structures can exhibit properties distinct from those of their single-crystal counterparts, owing to a large defect-to-volume ratio.[9,10] For example, Tang and Ouyang have shown that twin boundaries can serve as nanoscale channels for inward and outward transport of atoms within a silver nanocrystal.[9c] Lu et al. have shown that high-density nanoscale twins in a copper foil can effectively block dislocation motion, allowing a tenfold improvement in the mechanical strength relative to a large-grained copper sample.[9b] The lattice strain caused by twin defects also has a significant impact on the electronic structure of metal nanocrystals by altering the interatomic distances and thus the energy levels of bonding electrons, which in turn determines the catalytic and optical properties.[10] In general, controlling the twin structures of metal nanocrystals is crucial to tailoring their shapes and thus their properties and applications.

Both palladium and platinum are noble metals that crystallize with a face-centered cubic (fcc) packing, and they can form continuous solid solutions for all compositions.[11] Alloy nanocrystals made of Pd and Pt are of particular interest owing to their wide applications in catalytic and electrocatalytic reactions.[12] To date, various techniques have been developed to synthesize Pd–Pt alloy nanocrystals, which involved co-reduction of Pd and Pt precursors with alcohol or $NaBH_4$ as a reducing agent, laser ablation of bulk Pd–Pt alloys, and electrolysis in the presence of sacrificial bulk Pd and Pt electrodes.[13] However, the major products of all these syntheses have been restricted to small nanoparticles (typically less than 5 nm in size) with poorly defined crystallinity and morphology. The influence of twin defects on the evolution of shape and thus properties of Pd–Pt alloy nanocrystals remains largely unexplored.

It has been shown by simulation that Pd–Pt alloy clusters may adopt shapes different from those corresponding to either pure Pd or Pt clusters, such as incomplete or star-shaped decahedrons.[12d,14] However, these kinds of twinned structures for Pd–Pt alloys have never been observed in synthesis. Herein we demonstrate, for the first time, that Pd–Pt alloy nanocrystals with well-defined twinned structures can be synthesized by simple co-reduction of Na_2PdCl_4 and K_2PtCl_4 with poly(vinyl pyrrolidone) (PVP) in aqueous solution. Commercially available PVP (if it is synthesized in an aqueous medium) can serve as a weak reducing agent owing to its hydroxy (OH) end groups.[7a] Interestingly, we found that the resultant Pd–Pt alloy nanocrystals exhibited two different types of twinned structures: star-shaped decahedrons and triangular nanoplates with truncation at twin boundaries. We also demonstrated that the crystal structure of the alloy nanocrystals could be controlled by manipulating the reduction kinetics.

The synthesis was conducted in an aqueous solution containing Na_2PdCl_4, K_2PtCl_4, and PVP at 80 °C for 18 h, with a 1:1 molar ratio of Na_2PdCl_4 to K_2PtCl_4. A typical transmission electron microscopy (TEM) image of the product is shown in Figure 1a. The sample mainly contained star-shaped decahedrons with an average size of 40 nm (ca. 45% yield) and triangular nanoplates with lateral dimensions of 30–50 nm (50%) as well as a small fraction of other shapes, such as octahedrons (ca. 5%). A star-shaped decahedron can be described as a truncated decahedron in which the truncation reaches the maximum, thus producing a star-shaped profile (Supporting Information, Figure S1). The presence of fivefold twinning from the center of a star-shaped decahedron can be seen in Figure 1b. A star-shaped decahedron had a rhombic shape when viewed from the side (Supporting Information, Figure S2). On the other hand, the triangular nanoplates displayed two differently projected shapes under TEM, namely a triangle and a rectangle, depending on their orientation relative to the electron beam (Figure 1c,d). The TEM images also revealed truncation at the corners of the nanoplates. The overall weight percentage of Pt in this sample containing both types of twinned structures was 32%, as determined by inductively coupled plasma mass spectrometry (ICP-MS) measurements, which corresponds to a composition of $Pd_{80}Pt_{20}$.

[*] Dr. B. Lim, P. H. C. Camargo, C. M. Cobley, Prof. Y. Xia
Department of Biomedical Engineering, Washington University
St. Louis, MO 63130 (USA)
E-mail: xia@biomed.wustl.edu
Dr. J. G. Wang, Prof. M. J. Kim
Department of Materials Science, University of Texas at Dallas
Richardson, TX 75083 (USA)

[**] This work was supported in part by a research grant from NSF (DMR-0805088) and startup funds from Washington University in St. Louis. B.L. was also partially supported by a postdoctoral fellowship from the Korea Research Foundation funded by the Korean Government (KRF-2006-352-D00067). J.G.W. was supported by a grant from CNMT (08K1501-01210). P.H.C.C. was also supported in part by the Fulbright Program and the Brazilian Ministry of Education (CAPES).

Supporting information for this article is available on the WWW under http://dx.doi.org/10.1002/anie.200902235.

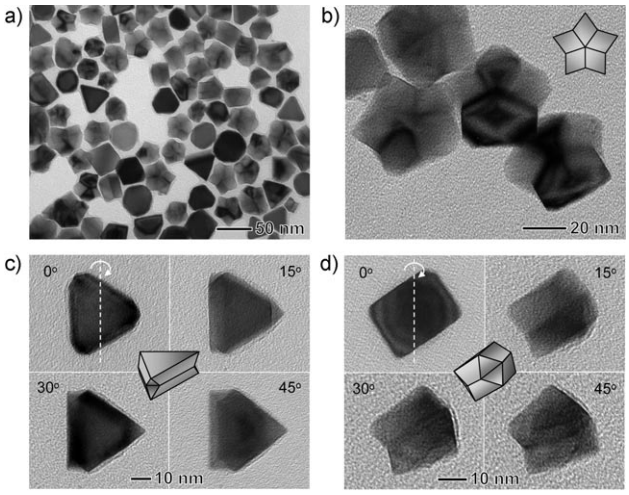

Figure 1. a) TEM image of Pd–Pt alloy nanocrystals synthesized by co-reduction of Na_2PdCl_4 and K_2PtCl_4 with PVP in an aqueous solution. The reaction was conducted at 80 °C for 18 h, with the molar ratio of Na_2PdCl_4 to K_2PtCl_4 at 1:1. Magnified TEM images of b) star-shaped decahedrons and c,d) triangular nanoplates tilted at different angles.

We further characterized the star-shaped decahedrons by high-angle annular dark-field scanning transmission electron microscopy (HAADF-STEM) and energy-dispersive X-ray spectroscopy (EDS) line scanning analyses (Figure 2a). The

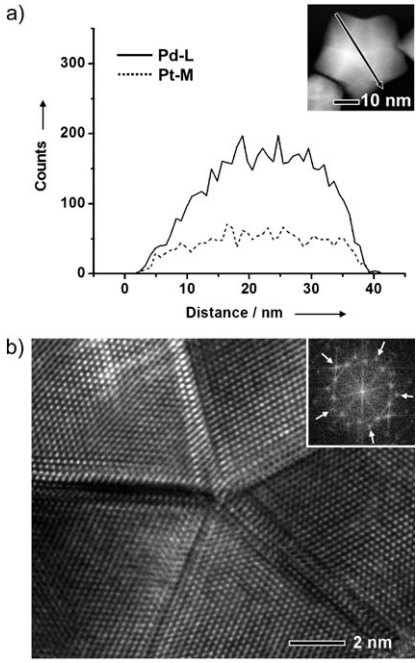

Figure 2. a) Compositional line profiles of Pd and Pt from a Pd–Pt alloy star-shaped decahedron recorded along the line shown in the HAADF-STEM image (inset). Pd-L and Pt-M refer to the L and M electron shells of the Pd and Pt atoms, respectively. The profiles were obtained by plotting the integrated intensities at Pd L-shell and Pt M-shell ionization edges. b) HRTEM image taken from the center of the star-shaped decahedron recorded along the [011] zone axis and the corresponding FT pattern (inset). In the FT pattern, the spots indicated by arrows can be indexed as the {200} reflections from five single-crystalline domains.

compositional line profiles of Pd and Pt on a star-shaped decahedron indicated that it was indeed a Pd–Pt alloy without significant segregation of each component. A high-resolution TEM (HRTEM) image taken from the center of the star-shaped decahedron clearly showed that it was composed of five single-crystalline domains with a twin-based adjoining plane between two neighboring domains (Figure 2b). The fivefold pentagonal symmetry can also be seen in the corresponding Fourier transform (FT) pattern (Figure 2b, inset).

Figure 3a,b shows the compositional line profiles recorded along the top and side faces of a Pd–Pt alloy nanoplate. It is clear that the two atomic species (i.e., Pd and Pt) are distributed homogeneously on the nanoplate to form a single phase. An HRTEM image taken from the top face of a nanoplate revealed the hexagonal arrangement of surface atoms with a lattice spacing of 1.38 Å (Figure 3c). The corresponding FT pattern showed an array of spots with sixfold rotational symmetry, which can be indexed as the {220} reflections (Figure 3c, inset).[15] These results indicate that the top and bottom faces of the nanoplate are enclosed by the {111} surfaces.[2a,6,7] An HRTEM image taken from the side face of a nanoplate revealed that there was a single {111} twin plane parallel to its top and bottom faces (Figure 3d).

In our synthesis, the slow reduction rate associated with the weak reducing power of PVP is a prerequisite for the formation of Pd–Pt alloy nanocrystals with twinned structures. We also conducted the reaction at a relatively high rate of co-reduction by using ethylene glycol (EG) as a reducing agent (i.e., the so-called polyol synthesis) instead of PVP, with the molar ratio of Na_2PdCl_4 to K_2PtCl_4 kept at 1:1. TEM images of the typical product are shown in Figure 4a,b. The product contained mainly nanocrystals with a nearly spherical profile and a mean diameter of about 6 nm. An HRTEM image of a single nanocrystal and the corresponding FT pattern revealed that it was a piece of single crystal with a truncated octahedral shape enclosed by a mix of {111} and {100} planes (Figure 4c). The HAADF-STEM and EDS line scanning analyses confirmed its composition as a Pd–Pt alloy (Figure 4d). The overall weight percentage of Pt determined by ICP-MS measurements was 61%, which corresponds to a composition of $Pd_{54}Pt_{46}$. These results clearly indicate that a fast reduction process favors the formation of Pd–Pt alloy nanocrystals with a single-crystal structure and a composition close to the feeding ratio.

Nanocrystals have been generally considered to grow by atomic addition. However, recent experimental and theoretical studies have shown that particle coalescence can also play an important role in nanocrystal growth.[16] We found that in the PVP-mediated synthesis the growth proceeded by particle coalescence. Figure 5a–e shows TEM images of samples taken from the reaction solution at 15 min, 30 min, 1 h, 3 h, and 8 h, respectively. At the early stages of the reaction, a large number of small particles (less than 3 nm) emerged, and some of them coalesced into single large particles with sizes of 10–20 nm (Figure 5a,b). The coalesced particles had either multiply or singly twinned structures (Supporting Information, Figure S3), indicating that twin defects were likely introduced by the coalescence of small particles. Recent

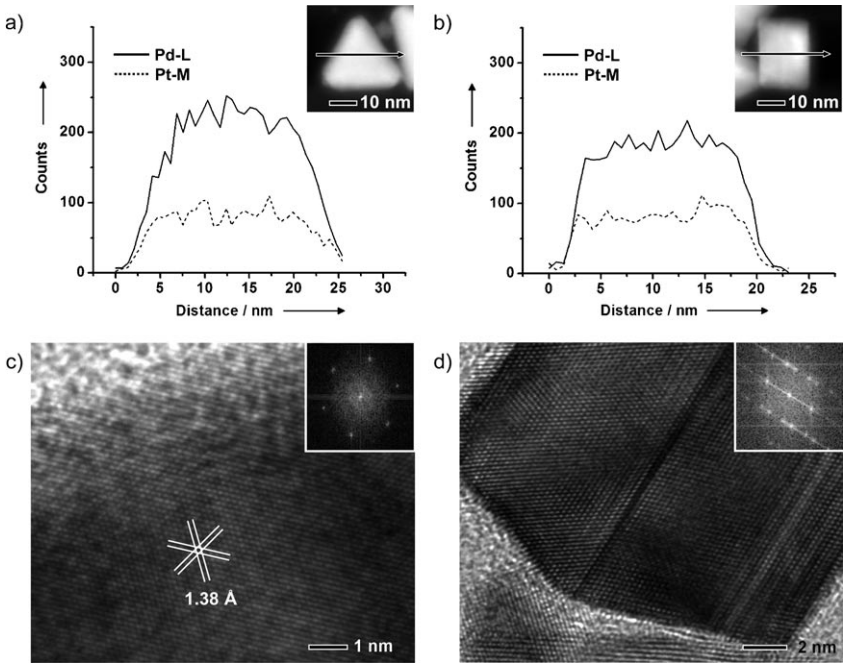

Figure 3. a,b) Compositional line profiles of Pd and Pt from the top and side faces of Pd–Pt alloy nanoplates recorded along the lines shown in the HAADF-STEM images (insets), respectively. c,d) HRTEM images taken from the top and side faces, respectively, of the nanoplates and the corresponding FT patterns (insets).

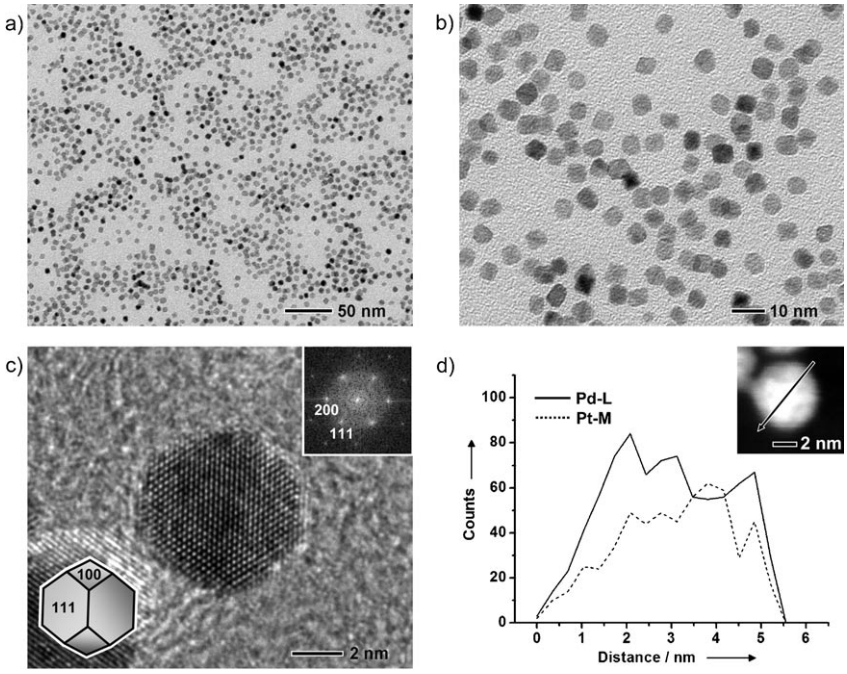

Figure 4. a,b) TEM images of Pd–Pt alloy nanocrystals synthesized by co-reducing Na_2PdCl_4 and K_2PtCl_4 with EG as a reducing agent. The reaction was conducted at 110°C for 5 h, with the molar ratio of Na_2PdCl_4 to K_2PtCl_4 at 1:1. c) HRTEM image of a single truncated octahedron shown in (a) recorded along the [011] zone axis. The insets show the corresponding FT pattern (upper right) and the geometrical model of the truncated octahedron (lower left). d) Compositional line profiles of Pd and Pt from the truncated octahedron recorded along the line shown in the HAADF-STEM image (inset).

molecular dynamics simulation has shown that coalescence events between fcc-structured clusters with surfaces that are partially bounded by stacking faults can generate twinned nuclei.[17] We have now experimentally observed such phenomena. The twinned particles could serve as seeds for further growth. As shown in Figure 5 c–e, the number of small particles decreased with prolonged reaction time, and large twinned particles kept growing by means of surface attachment and subsequent recrystallization of small particles. In contrast, we observed the formation of faceted nanocrystals with relatively large sizes of 6–7 nm at the early stage of the reaction in the polyol synthesis (Figure 5 f). These nanocrystals were dominated by an octahedral morphology (Supporting Information, Figure S4).

In the PVP-mediated synthesis, the generation and addition of metal atoms is slow so that particles formed by nucleation remain small for a long period of time.[2g] These small particles have a higher chemical potential owing to a larger surface-to-volume ratio and thus are easier to coalesce. The coalescence events between small particles give rise to an abrupt increase in particle size, along with twinning. In the polyol synthesis, however, the degree of initial supersaturation drastically increases owing to the fast reduction of metal precursors by EG,[2c,f] which leads to the rapid growth of the nuclei.[18] For an fcc metal, the surface energies of the low-index crystallographic facets that typically encase a nanocrystal are on the order of $\gamma\{111\} < \gamma\{100\} < \gamma\{110\}$. Accordingly, the nuclei tend to evolve into polyhedral structures such as octahedrons in an attempt to maximize the expression of {111} facets with the lowest surface energy. However, this shape has a larger surface area than a cube of the same volume. The dissolution of the corners of an octahedron produces a truncated octahedral shape (so-called Wulff polyhedron) that is more favored in terms of total surface energy per volume,[19] even though the octahedral shape was rapidly formed at an early stage of the reaction.

Regular decahedrons have been observed for Pd, Ag, and Au.[3] It is known that a solid-angle deficiency gives rise to internal lattice strain in a decahedral particle.[3,20] As the size increases, the lattice strain becomes significant and stress-release mechanisms such as faceting,

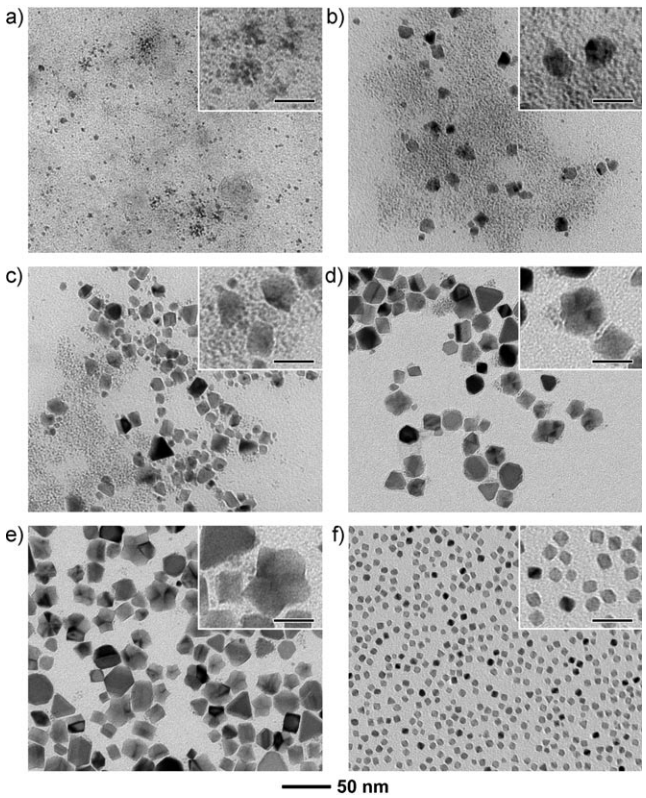

Figure 5. a–e) TEM images of Pd–Pt samples prepared under the same conditions as those in Figure 1a except that the reaction time was shortened to a) 15 min, b) 30 min, c) 1 h, d) 3 h, and e) 8 h. f) TEM image of a Pd–Pt sample prepared under the same conditions as those in Figure 4a except that the reaction time was shortened to 15 min. The scale bars in the insets correspond to 20 nm.

dislocation, and axis splitting begin to operate.[21] Among these mechanisms, faceting provides an effective means for minimizing both the strain and total surface energies of a nanocrystal. In the present system, a Pd–Pt alloy decahedron would have a higher surface energy than a pure Pd decahedron with the same size because Pt has a higher surface energy than Pd (see Table S1 in the Supporting Information).[22] The extra surface energy introduced by Pt atoms could result in an even higher faceting tendency for Pd–Pt alloy decahedrons in an effort to stabilize the entire structure, thus promoting their evolution into star-shaped decahedrons with maximum truncation at twin boundaries. This type of truncation provides the star-shaped decahedron with additional {111} facets.[20,21] Similarly, this relaxation mechanism based on faceting may also account for truncation in Pd–Pt alloy nanoplates. In this way, the structural stress caused by lamellar twins could be released efficiently.

In summary, we have demonstrated the synthesis of new types of Pd–Pt alloy nanocrystals, that is, star-shaped decahedrons and truncated triangular nanoplates, by a simple co-reduction route. The control over crystal structure and thus the final shape of a Pd–Pt alloy nanocrystal was achieved by manipulating the reduction kinetics by using different reducing agents such as PVP and EG. The evolution of twinned structures involves coalescence between initially formed small particles under slow reduction, in which the weak reducing power of PVP plays a critical role. We expect that the results presented herein will open the door to a systematic study of the shape control and properties of Pd–Pt alloy nanocrystals. More generally, this work provides a better understanding of twin formation and growth mechanisms involved in a kinetically controlled co-reduction synthesis.

Experimental Section

In a typical synthesis of Pd–Pt alloy nanocrystals with twinned structures, poly(vinyl pyrrolidone) (PVP, 35 mg, MW ≈ 55000, Aldrich) was dissolved in deionized water (8 mL) and heated to 80 °C in air under magnetic stirring. Meanwhile, sodium tetrachloropalladate(II) (Na_2PdCl_4, 9.5 mg, 0.032 mmol, Aldrich) and potassium tetrachloroplatinate(II) (K_2PtCl_4, 13.4 mg, 0.032 mmol, Aldrich) were co-dissolved in deionized water (3 mL) at room temperature. The aqueous solution of Na_2PdCl_4 and K_2PtCl_4 was then added dropwise to the PVP solution. The reaction mixture was heated at 80 °C in air for 18 h. In the synthesis of Pd–Pt alloy truncated octahedrons, PVP (105 mg) was dissolved in ethylene glycol (EG, 8 mL) and heated to 110 °C in air under magnetic stirring. Meanwhile, Na_2PdCl_4 (28.5 mg, 0.097 mmol) and K_2PtCl_4 (40.4 mg, 0.097 mmol) were co-dissolved in EG (3 mL) at room temperature. The EG solution of Na_2PdCl_4 and K_2PtCl_4 was then added dropwise to the PVP solution. The reaction mixture was heated at 110 °C in air for 5 h.

Transmission electron microscopy (TEM) images were captured using a Phillips 420 microscope operated at 120 kV. High-angle annular dark-field scanning TEM (HAADF-STEM) and high-resolution TEM (HRTEM) images were recorded with a JEOL 2100F microscope operated at 200 kV. The composition of Pd–Pt alloy nanocrystals was determined by inductively coupled plasma mass spectrometry (ICP-MS 7500CS, Agilent Technologies).

Received: April 27, 2009
Revised: June 17, 2009
Published online: July 20, 2009

Keywords: alloys · nanocrystals · palladium · platinum · twin defects

[1] a) N. Tian, Z.-Y. Zhou, S.-G. Sun, Y. Ding, Z. L. Wang, *Science* **2007**, *316*, 732; b) S. E. Habas, H. Lee, V. Radmilovic, G. A. Somorjai, P. Yang, *Nat. Mater.* **2007**, *6*, 692; c) B. Lim, X. Lu, M. Jiang, P. H. C. Camargo, E. C. Cho, E. P. Lee, Y. Xia, *Nano Lett.* **2008**, *8*, 4043; d) X. Lu, M. Rycenga, S. E. Skrabalak, B. Wiley, Y. Xia, *Annu. Rev. Phys. Chem.* **2009**, *60*, 167; e) J. Chen, B. Lim, E. P. Lee, Y. Xia, *Nano Today* **2009**, *4*, 81; f) B. Lim, M. Jiang, P. H. C. Camargo, E. C. Cho, J. Tao, X. Lu, Y. Zhu, Y. Xia, *Science* **2009**, *324*, 1302.

[2] a) C. Lofton, W. Sigmund, *Adv. Funct. Mater.* **2005**, *15*, 1197; b) J. L. Elechiguerra, J. Reyes-Gasga, M. J. Yacaman, *J. Mater. Chem.* **2006**, *16*, 3906; c) B. Wiley, Y. Sun, Y. Xia, *Acc. Chem. Res.* **2007**, *40*, 1067; d) S. Maksimuk, X. Teng, H. Yang, *J. Phys. Chem. C* **2007**, *111*, 14312; e) M. Tsuji, P. Jiang, S. Hikino, S. Lim, R. Yano, S.-M. Jang, S.-H. Yoon, N. Ishigami, X. Tang, K. S. N. Kamarudin, *Colloids Surf. A* **2008**, *317*, 23; f) Y. Xia, Y. Xiong, B. Lim, S. E. Skrabalak, *Angew. Chem.* **2009**, *121*, 62; *Angew. Chem. Int. Ed.* **2009**, *48*, 60; g) B. Lim, M. Jiang, J. Tao, P. H. C. Camargo, Y. Zhu, Y. Xia, *Adv. Funct. Mater.* **2009**, *19*, 189.

[3] a) L. D. Marks, A. Howie, *Nature* **1979**, *282*, 196; b) A. Sánchez-Iglesias, I. Pastoriza-Santos, J. Pérez-Juste, B. Rodríguez-González, F. J. G. de Abajo, L. M. Liz-Marzán, *Adv. Mater.* **2006**, *18*, 2529; c) Y. Gaoa, P. Jiangb, L. Songa, J. X. Wanga, L. F. Liua,

D. F. Liua, Y. J. Xianga, Z. X. Zhanga, X. W. Zhaoa, X. Y. Doua, S. D. Luoa, W. Y. Zhoua, S. S. Xie, *J. Cryst. Growth* **2006**, *289*, 376; d) B. Lim, Y. Xiong, Y. Xia, *Angew. Chem.* **2007**, *119*, 9439; *Angew. Chem. Int. Ed.* **2007**, *46*, 9279; e) C. L. Johnson, E. Snoeck, M. Ezcurdia, B. Rodríguez-González, I. Pastoriza-Santos, L. M. Liz-Marzán, M. J. Hÿtch, *Nat. Mater.* **2008**, *7*, 120; f) D. Seo, C. I. Yoo, I. S. Chung, S. M. Park, S. Ryu, H. Song, *J. Phys. Chem. C* **2008**, *112*, 2469; g) B. Pietrobon, V. Kitaev, *Chem. Mater.* **2008**, *20*, 5186.

[4] a) F. Kim, S. Connor, H. Song, T. Kuykendall, P. Yang, *Angew. Chem.* **2004**, *116*, 3759; *Angew. Chem. Int. Ed.* **2004**, *43*, 3673; b) Y. Xiong, J. M. McLellan, Y. Yin, Y. Xia, *Angew. Chem.* **2007**, *119*, 804; *Angew. Chem. Int. Ed.* **2007**, *46*, 790; c) K. Kwon, K. Y. Lee, Y. W. Lee, M. Kim, J. Heo, S. J. Ahn, S. W. Han, *J. Phys. Chem. C* **2007**, *111*, 1161; d) J. Xu, S. Li, J. Weng, X. Wang, Z. Zhou, K. Yang, M. Liu, X. Chen, Q. Cui, M. Cao, Q. Zhang, *Adv. Funct. Mater.* **2008**, *18*, 277.

[5] a) B. J. Wiley, Y. Xiong, Z.-Y. Li, Y. Yin, Y. Xia, *Nano Lett.* **2006**, *6*, 765; b) M. McEachran, V. Kitaev, *Chem. Commun.* **2008**, 5737.

[6] a) R. Jin, Y. Cao, C. A. Mirkin, K. L. Kelly, G. C. Schatz, J. G. Zheng, *Science* **2001**, *294*, 1901; b) S. S. Shankar, A. Rai, B. Ankamwar, A. Singh, A. Ahmad, M. Sastry, *Nat. Mater.* **2004**, *3*, 482; c) Q. Zhang, J. Ge, T. Pham, J. Goebl, Y. Hu, Z. Lu, Y. Yin, *Angew. Chem.* **2009**, *121*, 3568; *Angew. Chem. Int. Ed.* **2009**, *48*, 3516.

[7] a) I. Washio, Y. Xiong, Y. Yin, Y. Xia, *Adv. Mater.* **2006**, *18*, 1745; b) Y. Xiong, I. Washio, J. Chen, H. Cai, Z.-Y. Li, Y. Xia, *Langmuir* **2006**, *22*, 8563; c) Y. Xiong, I. Washio, J. Chen, M. Sadilek, Y. Xia, *Angew. Chem.* **2007**, *119*, 5005; *Angew. Chem. Int. Ed.* **2007**, *46*, 4917; d) B. Lim, P. H. C. Camargo, Y. Xia, *Langmuir* **2008**, *24*, 10437; e) B. Lim, J. Wang, P. H. C. Camargo, M. Jiang, M. J. Kim, Y. Xia, *Nano Lett.* **2008**, *8*, 2535.

[8] a) Y. Sun, Y. Xia, *Science* **2002**, *298*, 2176; b) Y. Xiong, J. Chen, B. Wiley, Y. Xia, S. Aloni, Y. Yin, *J. Am. Chem. Soc.* **2005**, *127*, 7332; c) C. Wang, H. Daimon, T. Onodera, T. Koda, S. Sun, *Angew. Chem.* **2008**, *120*, 3644; *Angew. Chem. Int. Ed.* **2008**, *47*, 3588.

[9] a) M. Chen, E. Ma, K. J. Hemker, H. Sheng, Y. Wang, X. Cheng, *Science* **2003**, *300*, 1275; b) L. Lu, Y. Shen, X. Chen, L. Qian, K. Lu, *Science* **2004**, *304*, 422; c) Y. Tang, M. Ouyang, *Nat. Mater.* **2007**, *6*, 754; d) K.-C. Chen, W.-W. Wu, C.-N. Liao, L.-J. Chen, K. N. Tu, *Science* **2008**, *321*, 1066; e) R. E. Algra, M. A. Verheijen, M. T. Borgström, L.-F. Feiner, G. Immink, W. J. P. van Enckevort, E. Vlieg, E. P. A. M. Bakkers, *Nature* **2008**, *456*, 369.

[10] a) J. Bao, D. C. Bell, F. Capasso, J. B. Wagner, T. Mårtensson, J. Trägårdh, L. Samuelson, *Nano Lett.* **2008**, *8*, 836; b) A. M. Smith, A. M. Mohs, S. Nie, *Nat. Nanotechnol.* **2009**, *4*, 56.

[11] F. R. De Boer, R. Boom, W. C. M. Mattens, A. R. Miedama, A. K. Niessen, *Cohesion in Metals: Transition Metal Alloys*, Elsevier, Amsterdam, **1988**.

[12] a) B. Coq, F. Figueras, *J. Mol. Catal. A* **2001**, *173*, 117; b) J. Zhang, M. B. Vukmirovic, Y. Xu, M. Mavrikakis, R. R. Adzic, *Angew. Chem.* **2005**, *117*, 2170; *Angew. Chem. Int. Ed.* **2005**, *44*, 2132; c) S. J. Yoo, H.-Y. Park, T.-Y. Jeon, I.-S. Park, Y.-H. Cho, Y.-E. Sung, *Angew. Chem.* **2008**, *120*, 9447; *Angew. Chem. Int. Ed.* **2008**, *47*, 9307; d) R. Ferrando, J. Jellinek, R. L. Johnston, *Chem. Rev.* **2008**, *108*, 845; e) Z. Peng, H. Yang, *Nano Today* **2009**, *4*, 143.

[13] a) N. Toshima, M. Harada, T. Yonezawa, K. Kushibashi, K. Asakurat, *J. Phys. Chem.* **1991**, *95*, 7448; b) A. Renouprez, J. L. Rousset, A. M. Cadrot, Y. Soldo, L. Stievano, *J. Alloys Compd.* **2001**, *328*, 50; c) H. Bönnemann, R. M. Richards, *Eur. J. Inorg. Chem.* **2001**, 2455; d) R. W. J. Scott, A. K. Datye, R. M. Crooks, *J. Am. Chem. Soc.* **2003**, *125*, 3708.

[14] a) C. Massen, T. V. Mortimer-Jones, R. L. Johnston, *J. Chem. Soc. Dalton Trans.* **2002**, 4375; b) L. D. Lloyd, R. L. Johnston, S. Salhi, N. T. Wilson, *J. Mater. Chem.* **2004**, *14*, 1691; c) G. Rossi, R. Ferrando, A. Rapallo, A. Fortunelli, B. C. Curley, L. D. Lloyd, R. L. Johnston, *J. Chem. Phys.* **2005**, *122*, 194309.

[15] D. B. Williams, C. B. Carter, *Transmission Electron Microscopy, Diffraction II*, Plenum, New York, **1996**, p. 282.

[16] a) J. Anwar, P. K. Boateng, *J. Am. Chem. Soc.* **1998**, *120*, 9600; b) J. F. Banfield, S. A. Welch, H. Z. Zhang, T. T. Ebert, R. L. Penn, *Science* **2000**, *289*, 751; c) C. Pacholski, A. Kornowski, H. Weller, *Angew. Chem.* **2002**, *114*, 1234; *Angew. Chem. Int. Ed.* **2002**, *41*, 1188; d) J. H. Yu, J. Joo, H. M. Park, S.-I. Baik, Y. W. Kim, S. C. Kim, T. Hyeon, *J. Am. Chem. Soc.* **2005**, *127*, 5662; e) M. Niederberger, H. Colfen, *Phys. Chem. Chem. Phys.* **2006**, *8*, 3271; f) M. A. Watzky, E. E. Finney, R. G. Finke, *J. Am. Chem. Soc.* **2008**, *130*, 11959; g) H. Zheng, R. K. Smith, Y.-w. Jun, C. Kisielowski, U. Dahmen, A. P. Alivisatos, *Science* **2009**, *324*, 1309.

[17] B. O'Malley, I. Snook, *Phys. Rev. Lett.* **2003**, *90*, 085702.

[18] a) V. K. LaMer, R. H. Dinegar, *J. Am. Chem. Soc.* **1950**, *72*, 4847; b) X. Peng, J. Wickham, A. P. Alivisatos, *J. Am. Chem. Soc.* **1998**, *120*, 5343; c) Z. A. Peng, X. Peng, *J. Am. Chem. Soc.* **2002**, *124*, 3343; d) Y. Yin, A. P. Alivisatos, *Nature* **2005**, *437*, 664; e) J. Park, J. Joo, S. G. Kwon, Y. Jang, T. Hyeon, *Angew. Chem.* **2007**, *119*, 4714; *Angew. Chem. Int. Ed.* **2007**, *46*, 4630.

[19] G. Z. Wulff, *Kristallogr. Mineral.* **1901**, *34*, 449.

[20] a) L. D. Marks, *Philos. Mag. A* **1984**, *49*, 81; b) H. Hofmeister, *Thin Solid Films* **1984**, *116*, 151; c) L. D. Marks, *Surf. Sci.* **1985**, *150*, 302; d) L. D. Marks, *Rep. Prog. Phys.* **1994**, *57*, 603649.

[21] M. J. Yacaman, J. A. Ascencio, H. B. Liu, J. Gardea-Torresdey, *J. Vac. Sci. Technol. B* **2001**, *19*, 1091.

[22] L. Vitos, A. V. Ruban, H. L. Skriver, J. Kollar, *Surf. Sci.* **1998**, *411*, 186.

